Received: 11 April 2024 | Accepted: 18 July 2024

DOI: 10.1002/pamm.202400006

PAMM Proceedings in Applied Mathematics and Mechanics

RESEARCH ARTICLE

A comparison of micromorphic gradient-extensions for anisotropic damage

Tim van der Velden[1] | **Tim Brepols**[1] | **Stefanie Reese**[1,2] | **Hagen Holthusen**[1]

[1]Institute of Applied Mechanics, RWTH Aachen University, Aachen, Germany

[2]University of Siegen, Siegen, Germany

Correspondence
Tim van der Velden, Institute of Applied Mechanics, RWTH Aachen University, Mies-van-der-Rohe-Str. 1, Aachen D-52074, Germany.
Email: tim.van.der.velden@ifam.rwth-aachen.de

Funding information
Deutsche Forschungsgemeinschaft, Grant/Award Numbers: 453715964, 495926269, 417002380(A01), 453596084(B05)

Abstract

The modeling of inelastic phenomena with tensor-valued internal variables requires a regularization to counteract mesh dependence. Here, we consider the regularization of anisotropic damage at finite strains and seek for an efficient formulation based on a reduced number of nonlocal degrees of freedom. We, thus, equip the brittle version of an anisotropic model with different gradient-extensions in the micromorphic framework using a full and a reduced regularization of the damage tensor. The models are compared in the structural simulation of an asymmetrically notched specimen with a perforated shear band section. High agreement is observed between the full and the reduced regularization with two nonlocal degrees of freedom. Furthermore, we present a novel study of the evolution of the reduced micromorphic field variables.

1 | INTRODUCTION

The localization of failure zones is a well-known problem in damage mechanics simulations [1, 2]. For the regularization of isotropic damage, numerous models have been developed that incorporate a nonlocal behavior by a regularization of the scalar damage variable. For the regularization of anisotropic damage, an efficient and yet accurate regularization of the damage tensor is the subject of current research. In ref. [3], we recently investigated the influence of different micromorphic gradient-extensions, which were applied to the same local anisotropic damage model, and we observed a high level of agreement between a strict and a reduced volumetric-deviatoric regularization (six versus two nonlocal degrees of freedom). In this contribution, we compare both regularizations for anisotropic damage on a new structural example with an a priori perforated failure zone to increase the complexity of the failure pattern.

Also for other inelastic phenomena, the regularization of tensor-valued internal variables is striven for with a minimum number of nonlocal variables, see for example, refs. [4, 5] for nonlocal plasticity. An efficient regularization of the inelastic phenomena is essential for their subsequent incorporation into multiphysics simulations, for example, refs. [6, 7], where additional fields are considered and the number of global variables is further increased.

2 | CONSTITUTIVE MODELING AND GRADIENT-EXTENSION

The anisotropic damage model utilized in this work corresponds to the brittle version of ref. [8], which is equipped with different gradient-extensions in ref. [3]. Here, we focus on the comparison of the strict regularization of the damage tensor with six nonlocal degrees of freedom to a reduced regularization of the damage tensor with two nonlocal degrees and retain the nomenclature of ref. [3], where model A denotes the strict regularization and model C the reduced volumetric-deviatoric regularization. Models A and C differ by the choice of the micromorphic tuple and the number of nonlocal degrees of freedom, but are based on the same local formulation, which is briefly summarized in the following:

- Helmholtz free energy

$$\psi\left(\boldsymbol{\eta}, \boldsymbol{D}, \xi_d, \mathbf{d}, \bar{\mathbf{d}}, \mathrm{Grad}\left(\bar{\mathbf{d}}\right)\right) = \underbrace{\psi_e\left(\boldsymbol{\eta}, \boldsymbol{D}\right)}_{\text{elasticity}} + \underbrace{\psi_d\left(\xi_d\right) + \psi_h\left(\boldsymbol{D}\right)}_{\text{isotropic and additional damage hardening}} + \underbrace{\psi_{\bar{d}}\left(\mathbf{d}, \bar{\mathbf{d}}, \mathrm{Grad}\left(\bar{\mathbf{d}}\right)\right)}_{\text{micromorphic gradient-extension}} \tag{1}$$

- State laws

$$\underbrace{\boldsymbol{\alpha} = \frac{\partial \psi}{\partial \boldsymbol{\eta}},}_{\text{mechanical stress}} \quad \underbrace{\xi_{0_i} = \frac{\partial \psi}{\partial \bar{\mathbf{d}}}, \quad \Xi_{0_i} = \frac{\partial \psi}{\partial \mathrm{Grad}\left(\bar{\mathbf{d}}\right)}}_{\text{generalized micromorphic stresses}} \tag{2}$$

- Damage loading function

$$\Phi_d := \sqrt{3}\sqrt{\boldsymbol{Y}_+ : \left((\boldsymbol{I} - \boldsymbol{D})^{c_d} \otimes (\boldsymbol{I} - \boldsymbol{D})^{c_d}\right)^{\overset{23}{\mathrm{T}}} : \boldsymbol{Y}_+} - (Y_0 - R_d) \leq 0 \tag{3}$$

- Evolution equations and loading / unloading conditions

$$\dot{\boldsymbol{D}} = \dot{\gamma}_d \frac{\partial \Phi_d}{\partial \boldsymbol{Y}}, \quad \dot{\xi}_d = \dot{\gamma}_d \frac{\partial \Phi_d}{\partial R_d}, \quad \dot{\gamma}_d \geq 0, \quad \Phi_d \leq 0, \quad \dot{\gamma}_d \Phi_d = 0 \tag{4}$$

- Micromorphic tuples

$$\mathbf{d}^{\mathrm{A}} = \left(D_{11}, D_{22}, D_{33}, D_{12}, D_{13}, D_{23}\right), \quad \mathbf{d}^{\mathrm{C}} = \left(\frac{\mathrm{tr}\left(\boldsymbol{D}\right)}{3}, \mathrm{tr}\left(\mathrm{dev}(\boldsymbol{D})^2\right)\right) \tag{5}$$

Here, $\boldsymbol{\eta}$ denotes a logarithmic strain measure with $\boldsymbol{\eta} = \ln(\boldsymbol{C})/2$, $\boldsymbol{D}$ a second order damage tensor, ξ_d the accumulated damage, $\mathbf{d}$ the local micromorphic tuple and $\bar{\mathbf{d}}$ its nonlocal counterpart, $\boldsymbol{Y}$ the damage driving force, and R_d the damage hardening driving force. For further details, the reader is kindly referred to refs. [3, 8].

3 | NUMERICAL EXAMPLE

Inspired by ref. [9], we investigate the following asymmetrically notched specimen with a perforated shear band section (Figure 1). The dimensions read $\ell = 110\,[\mathrm{mm}]$, $h = 30\,[\mathrm{mm}]$, $w = 10\,[\mathrm{mm}]$, $r = 3.5355\,[\mathrm{mm}]$ and the thickness is $1\,[\mathrm{mm}]$. Further, we employ plane strain conditions with Q1 elements, while the application of structural elements, for example, refs. [10–12], is aspired in future works. The material and numerical parameters read $\Lambda = 25000\,[\mathrm{MPa}]$, $\mu = 55000\,[\mathrm{MPa}]$, $Y_0 = 2.5\,[\mathrm{MPa}]$, $\vartheta = 1\,[-]$, $r_d = 5\,[\mathrm{MPa}]$, $s_d = 100\,[-]$, $H_d = 1\,[\mathrm{MPa}]$, $c_d = 1\,[-]$, $K_h = 0.1\,[\mathrm{MPa}]$, $n_h = 2\,[-]$, $a_h = 0.999999\,[-]$, $\eta_v = 1\,[\mathrm{MPas}]$, $H_i^{\mathrm{A,C}} = 10^4\,[\mathrm{MPa}]$. The gradient parameters of model A are chosen $A_i^{\mathrm{A}} = 300\,[\mathrm{MPa\,mm^2}]$ and of model C as $A_i^{\mathrm{C}} = 1030\,[\mathrm{MPa\,mm^2}]$ to obtain the same load bearing capacity, that is, the same maximum structural force response.

In Figure 2, the force-displacement curves of models A and C are presented for a mesh convergence study with different discretizations of 1235, 3122, 7571, and 10 143 elements. Both models yield a converged solution for the refined mesh with 3122 elements. Moreover, the structural responses of models A and C agree qualitatively and quantitatively well.

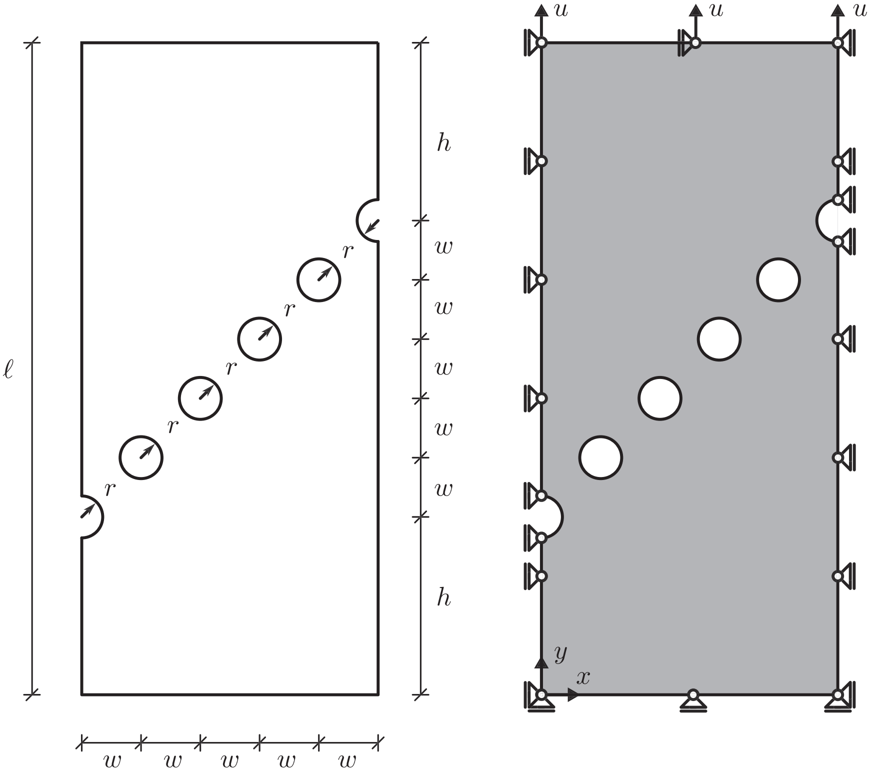

(A) Geometry (B) Boundary value problem

FIGURE 1 Geometry and boundary value problem of the asymmetrically notched specimen with perforated shear band section.

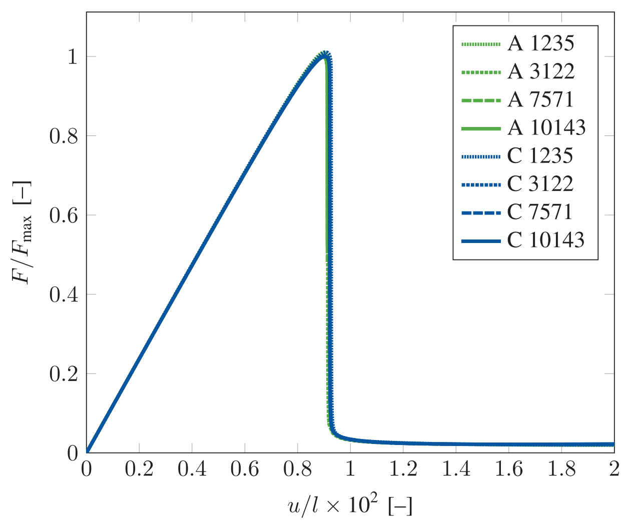

FIGURE 2 Mesh convergence study for the simulations of the asymmetrically notched specimen with perforated shear band section for model A and model C. The forces are normalized with respect to the maximum force of the finest mesh of model A (10 143 elements) with $F_{\max} = 5.0403 \times 10^4$ N.

In Figures 3 and 4, the evolution of the normal and shear components of the second order damage tensor for model A and model C is presented. The damage contour plots show an equal behavior for the normal components, D_{xx} and D_{yy}, for both models. Damage initiates in an inclined band between the left and right half notch along the perforated section, where the most pronounced evolution occurs between the outer half notches and the outermost full notches. Finally, the crack, that is, the completely damaged area of the specimen, forms between the notches with a diffuse damage zone below and above the notches.

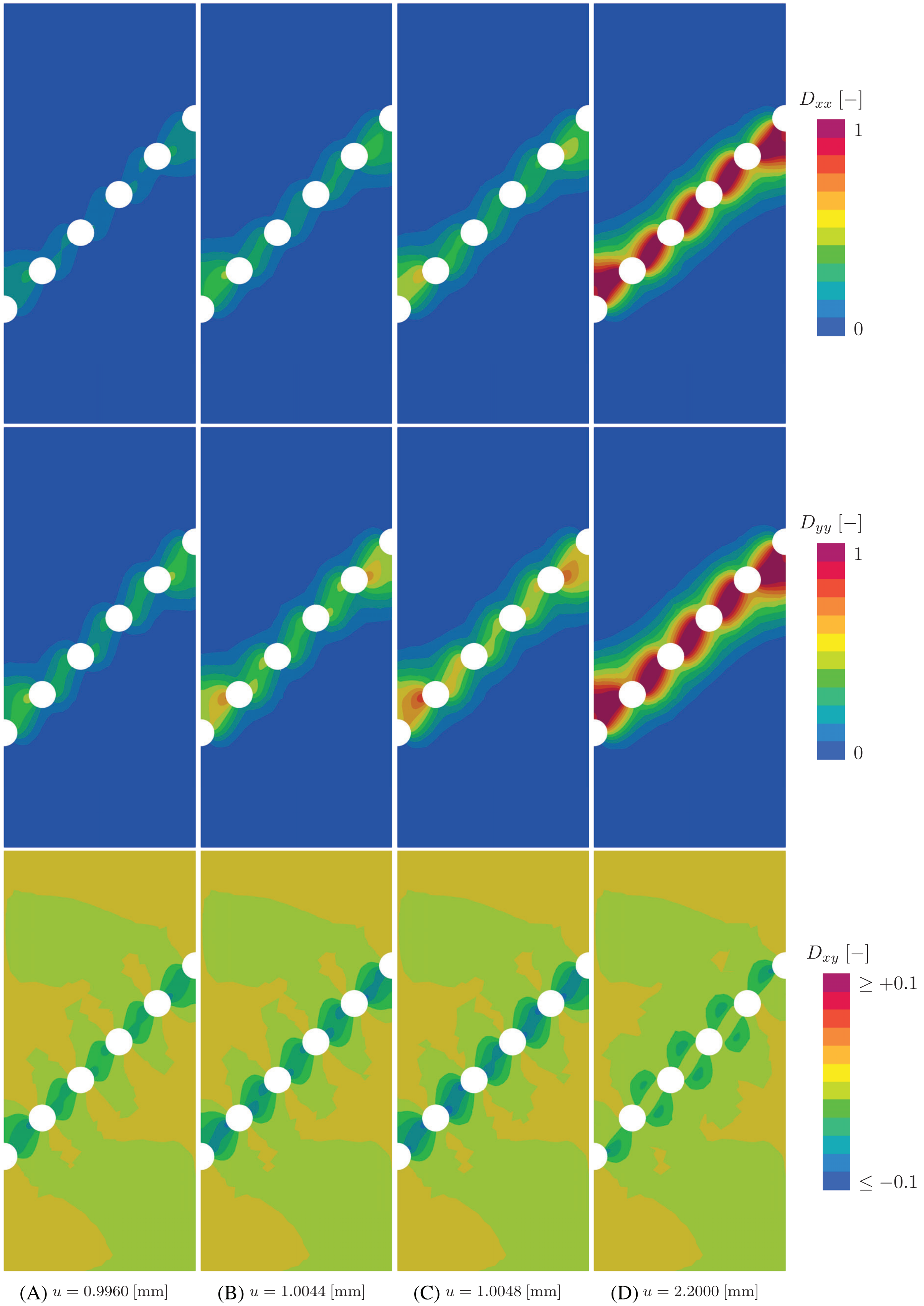

FIGURE 3 Evolution of the normal components D_{xx} and D_{yy} (top and middle row) and the shear component D_{xy} (bottom row) of the damage tensor $\boldsymbol{D}$ for model A.

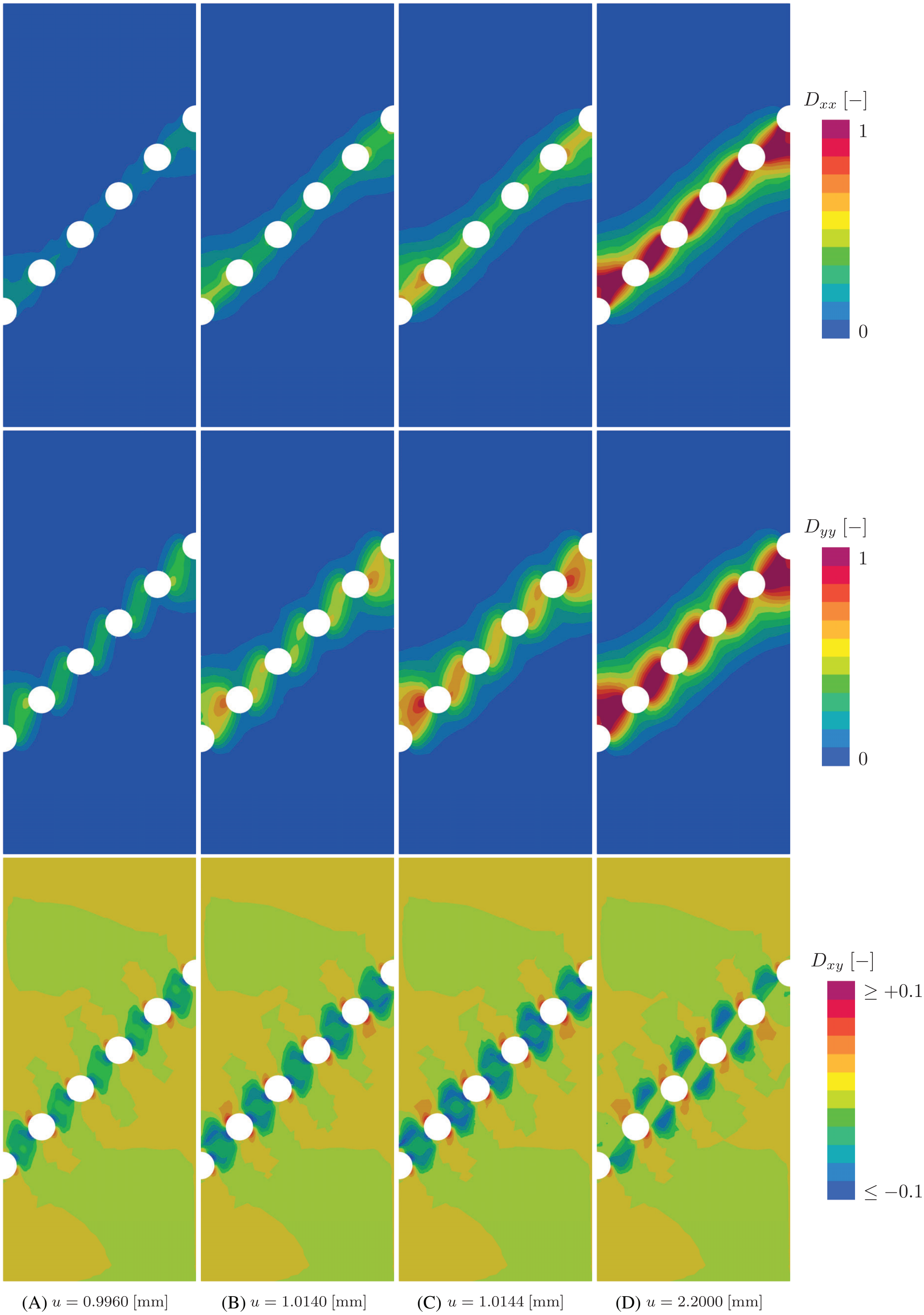

FIGURE 4 Evolution of the normal components D_{xx} and D_{yy} (top and middle row) and the shear component D_{xy} (bottom row) of the damage tensor $\boldsymbol{D}$ for model C.

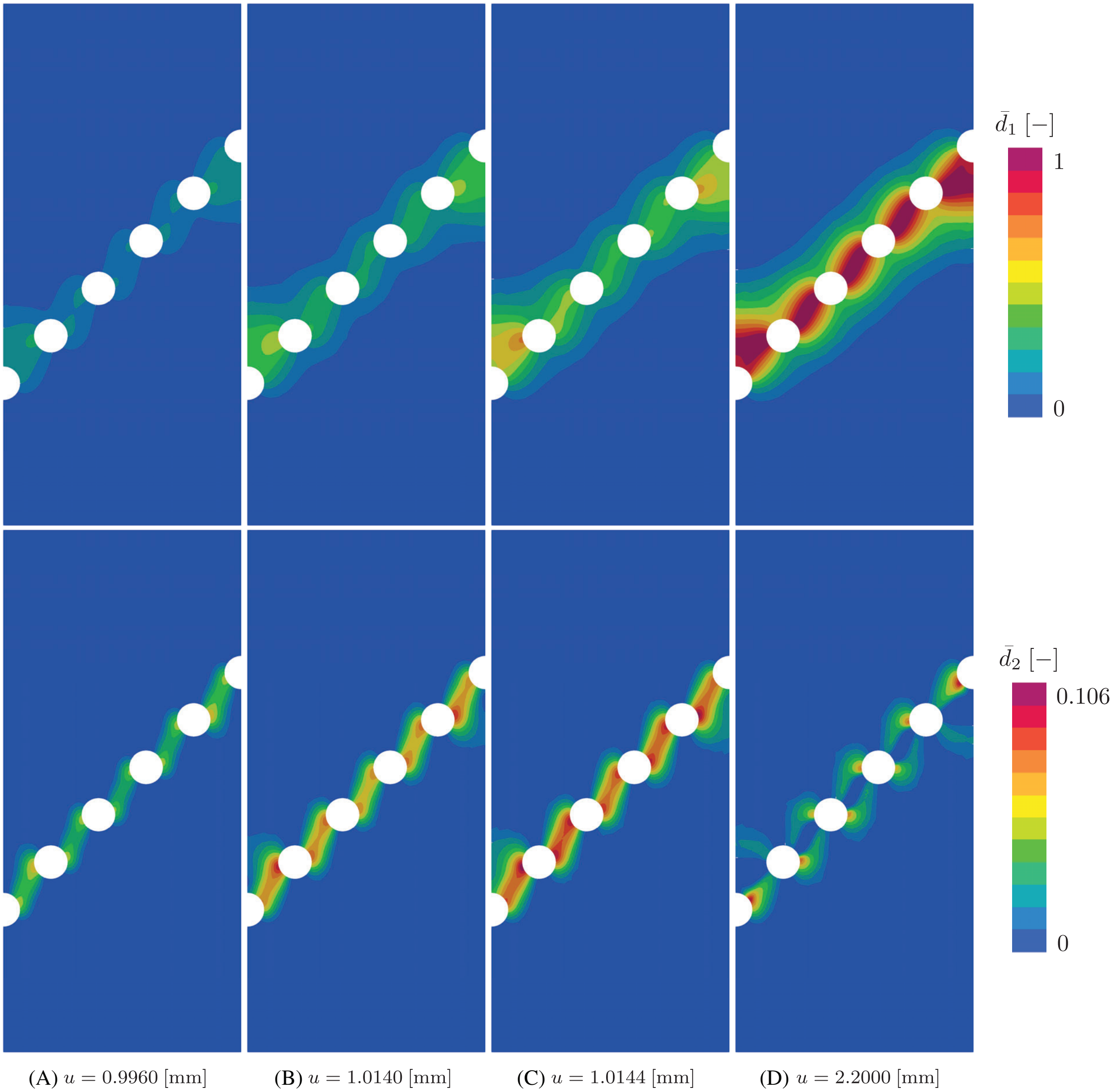

FIGURE 5 Evolution of the micromorphic nonlocal field variables $\bar{d}_1$ and $\bar{d}_2$ for model C.

The evolution of the shear components, D_{xy}, also shows a qualitatively similar damage pattern for model A (Figure 3) and model C (Figure 4). However, the maximum absolute value differs with $|D_{xy}^{\mathrm{A}}| = 0.081$ and $|D_{xy}^{\mathrm{C}}| = 0.114$ between both models around the notches.

Additionally, the evolution of the nonlocal micromorphic micromorphic degrees of freedom of model C is shown in Figure 5. A fully damaged state of the material corresponds to the identity, that is, $\boldsymbol{D} = \boldsymbol{I}$, and, hence, the maximum value of the first component of the micromorphic tuple, $\bar{d}_1 = \mathrm{tr}(\boldsymbol{D})/3$, yields for $\boldsymbol{D} = \boldsymbol{I}$ a value of $\bar{d}_1 = 1$ in the area of the crack.

The second component of the micromorphic tuple, $\bar{d}_2 = \mathrm{tr}(\mathrm{dev}(\boldsymbol{D})^2)$, initially grows and yields non-zero values in the entire shear band section, but finally for $\boldsymbol{D} = \boldsymbol{I}$, a value of $\bar{d}_2 = 0$ in the area of the crack is obtained.

4 | CONCLUSION

In this work, we applied an anisotropic damage model with two different gradient-extensions for the simulation of an asymmetrically notched specimen with a perforated shear band section. The gradient-extensions differ in their number of nonlocal degrees of freedom, six versus two, thereby, describing a full and a reduced regularization. The efficient reduced volumetric-deviatoric regularization yields results in close agreement with the full regularization and confirms the results of previous studies in ref. [3] on a new structural example. Furthermore, additional studies with respect to the evolution of the micromorphic variables are presented.

Currently, the model describes damage as induced anisotropy. In future works, we aim for the extension towards initial anisotropy analogously for example, refs. [13, 14]. Furthermore, the reduced model may be applied to the anisotropic damage modeling of paperboard [15, 16] and failure model identification with iCANNs [17].

ACKNOWLEDGMENTS

Funding granted by the Deutsche Forschungsgemeinschaft (DFG) for projects number 453715964, 495926269, 417002380 (A01), and 453596084 (B05) is gratefully acknowledged.

Open access funding enabled and organized by Projekt DEAL.

ORCID

Tim van der Velden https://orcid.org/0000-0001-8054-5091
Tim Brepols https://orcid.org/0000-0002-1039-1776
Hagen Holthusen https://orcid.org/0000-0002-0700-8027

REFERENCES

1. de Borst, R., Sluys, L. J., Mühlhaus, H. B., & Pamin, J. (1993). Fundamental issues in finite element analyses of localization of deformation. *Engineering Computations*, *10*(2), 99–121.
2. Rizzi, E., Carol, I., & Willam, K. (1995). Localization analysis of elastic degradation with application to scalar damage. *Journal of Engineering Mechanics*, *121*(4), 541–554.
3. van der Velden, T., Brepols, T., Reese, S., & Holthusen, H. (2023). A comparative study of micromorphic gradient-extensions for anisotropic damage at finite strains. *International Journal for Numerical Methods in Engineering*, e7580.
4. Abatour, M., Forest, S., Ammar, K., Ovalle, C., Osipov, N., & Quilici, S. (2023). Toward robust scalar-based gradient plasticity modeling and simulation at finite deformations. *Acta Mechanica*, *234*, 911–958.
5. Abatour, M., & Forest, S. (2023). Strain gradient plasticity based on saturating variables. *European Journal of Mechanics - A/Solids*, *104*, 105016.
6. van der Velden, T., Rommes, B., Klink, A., Reese, S., & Waimann, J. (2021). A novel approach for the efficient modeling of material dissolution in electrochemical machining. *International Journal of Solids and Structures*, *229*, 111106.
7. van der Velden, T., Ritzert, S., Reese, S., & Waimann, J. (2023). A novel numerical strategy for modeling the moving boundary value problem of electrochemical machining. *International Journal for Numerical Methods in Engineering*, *124*(8), 1856–1882.
8. Holthusen, H., Brepols, T., Reese, S., & Simon, J. W. (2022). A two-surface gradient-extended anisotropic damage model using a second order damage tensor coupled to additive plasticity in the logarithmic strain space. *Journal of the Mechanics and Physics of Solids*, *163*, 104833.
9. Pohl, T. (2014). *Adaptive Methoden zur Pfadverfolgung bei Entfestigung*. University of Stuttgart.
10. Barfusz, O., Brepols, T., van der Velden, T., Frischkorn, J., & Reese, S. (2021). A single gauss point continuum finite element formulation for gradient-extended damage at large deformations. *Computer Methods in Applied Mechanics and Engineering*, *373*, 113440.
11. Barfusz, O., van der Velden, T., Brepols, T., Holthusen, H., & Reese, S. (2021). A reduced integration-based solid-shell finite element formulation for gradient-extended damage. *Computer Methods in Applied Mechanics and Engineering*, *382*, 113884.
12. Barfusz, O., van der Velden, T., Brepols, T., & Reese, S. (2022). Gradient-extended damage analysis with reduced integration-based solid-shells at large deformations. *Computer Methods in Applied Mechanics and Engineering*, *389*, 114317.
13. Holthusen, H., Brepols, T., Reese, S., & Simon, J. W. (2020). An anisotropic constitutive model for fiber-reinforced materials including gradient-extended damage and plasticity at finite strains. *Theoretical and Applied Fracture Mechanics*, *108*, 102642.
14. Poggenpohl, L., Brepols, T., Holthusen, H., Wulfinghoff, S., & Reese, S. (2021). Towards brittle damage in carbon fiber reinforced plastics: A gradient extended approach. *Composite Structures*, *255*, 112911.
15. Alzweighi, M., Tryding, J., Mansour, R., Borgqvist, E., & Kulachenko, A. (2023). Anisotropic damage behavior in fiber-based materials: Modeling and experimental validation. *Journal of the Mechanics and Physics of Solids*, *181*, 105430.
16. Boes, B., Simon, J. W., Reese, S., & Holthusen, H. (2023). A novel continuum mechanical framework for decoupled material behavior in thickness and in-plane directions. *Computer Methods in Applied Mechanics and Engineering*, *415*, 116192.
17. Holthusen, H., Lamm, L., Brepols, T., Reese, S., & Kuhl, E. (2024). Theory and implementation of inelastic constitutive artificial neural networks. *Computer Methods in Applied Mechanics and Engineering*, *428*, 117063.

How to cite this article: van der Velden, T., Brepols, T., Reese, S., & Holthusen, H. (2024). A comparison of micromorphic gradient-extensions for anisotropic damage. *Proceedings in Applied Mathematics and Mechanics*, e202400006. https://doi.org/10.1002/pamm.202400006